

MICROSCOPIC MECHANISM OF THE GIANT ELECTORRHEOLOGICAL EFFECT

SHUYU CHEN, XIANXIANG HUANG, WEIJIA WEN and PING SHENG*

*Department of Physics and William Mong Institute of Nano Science and Technology,
Hong Kong University of Science and Technology, Clear Water Bay, Kowloon,
Hong Kong, China*

NICO F. A. VAN DER VEGT

*Center of Smart Interfaces, Technical University of Darmstadt,
Petersenstrasse 32, 64287 Darmstadt, Germany*

Electrorheological (ER) fluids are a type of colloids whose rheological characteristics can be varied reversibly with the application of an electric field. The traditional ER mechanism is based on induced polarization arising from the dielectric constant contrast between the suspended solid particles and the fluid. However, for induced polarization there is a maximum value for the dimensionless electric susceptibility $\chi \sim 0.24$. That implies an upper bound for the traditional ER effect. For permanent molecular dipoles, χ can be as high as 4-50. Thus, one to two orders of magnitude higher electric energy can be gained by harnessing the molecular dipoles. Indeed, the recent discovery of the giant electrorheological (GER) effect, in nanoparticles of urea-coated barium titanate oxalate suspended in silicone oil, has shown that the theoretical upper bound of the traditional ER effect is no longer applicable to this new type of electrorheological fluid. A phenomenological model of the GER mechanism, based on aligned molecular dipoles of urea molecules in the contact regions of the nanoparticles, yields an adequate account of the observed effect but without a microscopic picture on how this can occur. More recently, by using molecular dynamics (MD) to simulate the urea-silicone oil mixture confined between two bounding surfaces of a nanocontact, we find that the urea molecules, which has a molecular dipole moment of 4.6 Debye, can form aligned dipolar filaments that penetrate the oil film to bridge the two substrates, with the attendant lowering of the aligning field for the urea dipoles. This phenomenon is explainable on the basis of a 3D to 1D crossover in urea molecules' microgeometry, realized through the confinement effect provided by the oil chains. The resulting electrical energy density is shown to give an excellent account of the observed yield stress variation as a function of the electric field.

* Corresponding author: sheng@ust.hk

1. Introduction

1.1. Induced dipole vs. molecular dipole

Electrorheological (ER) fluid comprises of solid particles dispersed in an insulating liquid. The traditional ER effect is based on induced polarization under an applied electric field \vec{E} , caused by the dielectric constant contrast between the suspended solid particles and the liquid. There is an extensive literature on the traditional ER effect, see, e.g., R. Tao [1], D. J. Klingenberg [2], H. Conrad [3], G. Bossis [4], H. R. Ma et al. [5], and J. E. Martin et al. [6]. Reviews can be found in [7,8].

Let ϵ_s denote the complex dielectric constant of the solid particles and ϵ_l that of the liquid; then for spherically shaped particles, the induced dipole moment may be expressed as:

$$\vec{p} = \frac{\epsilon_s - \epsilon_l}{\epsilon_s + 2\epsilon_l} a^3 \vec{E} = \beta a^3 \vec{E}, \quad (1)$$

where a is the radius of the particles and β is the Clausius-Mossotti factor. The product $\beta a^3 = \alpha$ is denoted the polarizability. The (induced) dipole-dipole interaction between the particles means that the particles would tend to aggregate and form chains/columns along the applied field direction, leading to increased viscosity under shear. With increasing electric field the ER fluid may even turn into a weak solid characterizable by the existence of a yield stress that is proportional to the energy density $W = |-\vec{P} \cdot \vec{E}|$, where $\vec{P} = N\vec{p}$ is the polarization density, with N being the number density of the solid particles. The dependence of the yield stress on the electric field is necessarily quadratic. That is because for induced polarization $\vec{P} = \chi \vec{E}$, where $\chi = N\alpha$ is the dimensionless electric susceptibility. Hence $|-\vec{P} \cdot \vec{E}| = \chi E^2$. Also, since there is a maximum value of polarizability $\alpha = a^3$, reached at the limit of $\epsilon_s / \epsilon_l \rightarrow \infty$, it follows that there is a maximum value for the dimensionless electric susceptibility $\chi = N\alpha = a^3 / (4\pi a^3 / 3) \sim 0.24$. A more rigorous theory [7], based on the effective dielectric constant formulation of the ER problem, can give an upper bound for the yield stress, expressible as $1.38\sqrt{R/\delta}(\epsilon_l E^2 / 8\pi)$, with R the radius of the particles and δ the separation. Therefore, limited by the breakdown electric field, the yield stress achievable by most of the traditional ER effect is usually on the order of a few kPa.

Motivated by a desire to break the upper bound imposed by the induced polarization mechanism, the search naturally turns to permanent molecular dipoles, whose polarizability α_m differs from that expressed by Eq. (1) and is the result of competition between the alignment energy $-\vec{p}_0 \cdot \vec{E}$ and thermal Brownian motion, where p_0 denotes the molecular dipole moment. Since the dipole-field interaction energy is given by $-p_0 E \cos \theta$, where θ denotes the angle between the field and the dipole moment, the Boltzmann factor is given by $\exp(p_0 E \cos \theta / k_B T)$. In 3D, the average dipole moment is therefore given by the Langevin function:

$$\langle p \rangle = \frac{\int_0^\pi p_0 \cos \theta \exp(p_0 E \cos \theta / k_B T) \frac{1}{2} \sin \theta d\theta}{\int_0^\pi \exp(p_0 E \cos \theta / k_B T) \frac{1}{2} \sin \theta d\theta} = p_0 \left(\coth(x) - \frac{1}{x} \right), \quad (2)$$

where $x = p_0 E / k_B T$. For $p_0 = 4.6$ D and $T = 300$ K, $x = 1$ only when $E = 2.5 \times 10^6$ V/cm. For electric field much smaller than that, $\langle p \rangle \rightarrow (p_0^2 / 3k_B T) \vec{E}$ so that $\alpha_m = p_0^2 / 3k_B T$. That implies $\chi_m \sim 4-50$, depending on the number density we choose. Thus there can be at least one to two orders of magnitude to be gained if the molecular dipoles can indeed be harnessed.

1.2. Giant electrorheological effect and its phenomenological model

Persistent experimental efforts have led to the discovery of urea-coated nanoparticles of barium titanate oxalate ($\text{NH}_2\text{CONH}_2 \oplus \text{BaTiO}(\text{C}_2\text{O}_4)_2$) which, when dispersed in silicone oil, exhibits ER effect orders magnitude larger than those based on the induced polarization mechanism, exceeding the upper bound value by a large factor [9]. The GER effect also displays a *linear electric field dependence* of the yield stress, implying the GER mechanism must involve a polarization saturation phenomenon. It has also been observed that the GER effect scales as $1/R$, implying a surface-area dependence [10]. But perhaps the most intriguing aspect is that the GER effect is highly sensitive to whether the dispersing oil can wet the solid particles [11,12]. From such experimental observations it can be deduced that the GER effect involves some form of synergistic interaction between the urea molecules and the oil.

We have developed a phenomenological GER model [9,13] that is based on the following four elements. (1) There is an electric field enhancement effect at the contact region, with an enhancement factor on the order of $\sim 10^2$ (estimated numerically by using the finite element method). (2) The molecular dipoles of urea can form aligned dipolar layers in the *contact region* between two coated

nanoparticles, under a moderate microscopic electric field of 10^6 - 10^7 V/cm. (3) The equilibrium contact state is represented by the balance of the (attractive) electrostatic force with the (repulsive) elastic force; with the elastic deformation of two coated spheres in contact given by the Hertzian solution. (4) The shear stress is defined as the derivative of the total energy with respect to strain; and as the area of the contact region decreases under shear, the yield stress is given by the stress value at the point of separation (zero contact area).

In this model, there is only one adjustable parameter, given by the deformation modulus of the coating. It turns out that the value obtained from fitting the experimental data is ~ 0.1 GPa [13], similar to that for a liquid and agrees with the TEM observation that the coatings seem to be soft [9].

While the phenomenological model predicts both the linear dependence on the applied electric field as well as the surface area dependence on the magnitude of the effect (hence smaller particles would enhance the GER effect) [10], it fails to account (1) *how does the alignment of the molecular dipoles come about, and* (2) *what is the synergistic role of the silicone oil in the GER mechanism.* We have turned to the use of molecular dynamics (MD) simulation to seek a physical picture of the microscopic GER mechanism. In this paper, we show that in the contact region between two nanoparticles, urea molecules, which normally reside at the oil-particle interface, can form aligned dipolar filaments that penetrate the oil film to bridge the two substrates. The resulting electrical energy density is shown to give an excellent account of the observed yield stress variation as a function of the electric field.

2. Microscopic Mechanism of the GER Effect

We focus on the contact area of two spherical nanoparticles and model it with a 2.9 nm gap in which the (methyl-group terminated) silicone oil chains with 10 monomers per chain and urea molecules are sandwiched between two bounding surfaces populated by water molecules. Owing to the nonideal thermodynamic nature of the urea-water solution, it is known that urea molecules tend to predominantly aggregate at the surface of hydrophilic solid particles, forming a (nonuniform) liquid-like coating. MD simulations were performed with the package GROMACS. Details of the model and the methodology involved can be found in Ref. [14].

2.1. Observation of molecular filament formation

When the electric field was turned on, the urea molecules were seen to diffuse into the silicone oil layer from both sides, with their molecular dipoles generally

aligned along the field direction, forming filaments that bridge the two sides of the gap. Figure 1 shows a snapshot taken from the simulation to illustrate the configuration of the system under a 0.2 V/nm electric field. The filament structure may be clearly discerned in Fig. 1(a). In Fig. 1(b) we explicitly delineate the hydrogen bonds between the urea molecules in the filaments. A typical dipole moment in the filament is >3 D along the direction of the electric field. In contrast, with a homogenous dispersion of liquid-like urea molecule, it was found that it requires at least 0.6 V/nm of electric field in order to align the urea molecules. Thus there is clearly a lowering of the required electric field for dipole alignment by a factor of 2 to 3. The formation of the filaments always

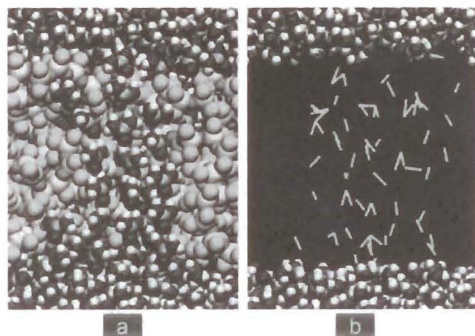


Figure 1. (a) Urea molecular filaments across silicone oil layer under 0.2 V/nm electric field. The methyl group is represented by a single green sphere. Oxygen, hydrogen, nitrogen, carbon, and silicon atoms are denoted by red, white, blue, navy blue, and yellow, respectively. Only part of the water boundary layer (red-white) is shown. (b) The hydrogen bondings (highlighted by bright yellow lines) between the urea molecules in the filament structure.

starts at the substrates, and no formation of filaments was ever observed in our simulations for gaps >10 nm. Thus the formation of filaments (and therefore the enhanced alignment) is inherently an interfacial effect with a decay length <4 – 5 nm. Figure 2(a) shows the results of varying the gap size and finding the field at which the filaments are no longer observed. It is seen that for large fields, the gap size saturates at 8–9 nm. This essentially sets a length scale for the GER effect. Owing to the small magnitude of this length scale, the GER effect may be considered an interfacial phenomenon, with its magnitude scaling [10] with the interfacial area.

2.2. Confinement effect and the 3D to 1D crossover

The formation of filaments, with the attendant lowering of the aligning field and the finite penetration length, may be attributed to the confinement effect exerted

by the oil chains, because of their hydrophobic nature. The confinement, which tends to decrease the entropic phase space of the urea dipoles, works in concert with the hydrogen bonding interactions (Fig. 1(b)) to significantly increase urea dipoles' sensitivity to the field. This effect may be mathematically formulated by noting that for 3D the thermally-averaged dipole moment along the field direction is given by Eq. (2), where for urea molecules $p_0 = 4.6$ Debye. But for 1D, it is given by $\langle p \rangle_{1D} / p_0 = \tanh(p_0 E / k_B T)$. At any given E , $\Delta p = \langle p \rangle_{1D} - \langle p \rangle_{3D}$ is *always positive*, as shown in Fig. 2(b); therefore $-\Delta p \cdot E$ provides a driving energy/force for the urea molecules to develop a more diffuse interface with the oil film, in the form of 1D filaments' penetration into the oil film (under an electric field). The presence of hydrogen bonds between the urea molecules in the filaments means that their energetic contributions (per urea

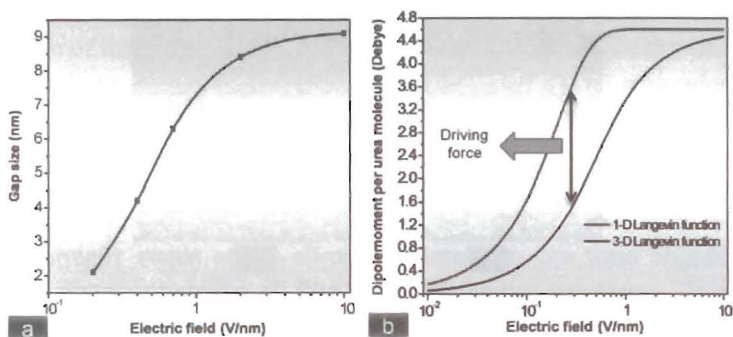


Figure 2. (a) Maximum thickness of the oil layer in the gap (beyond which no filament formation can be observed) plotted as a function of applied electric fields. (b) Dipole moment per urea molecule along the field direction as a function of field in 3D (black curve) and 1D (red curve). The difference provides a driving force for forming the molecular filaments.

molecule) can help to counterbalance those in the (3D) urea molecular dispersion. The electrical alignment energy thereby emerges as the dominant factor. Moreover, as $E \rightarrow \infty$, we have $\Delta p \rightarrow k_B T / E$, which implies $-\Delta p \cdot E$ approaches a constant value, $-k_B T$, independent of E . This is consistent with the saturation behavior as $E \rightarrow \infty$, seen in Fig 2(a). This behavior also confirms the surface scaling aspect of the GER effect.

2.3. Electrical energy density and comparison with GER data

To obtain the relation between the yield stress as a function of the electric field, we calculate the total electrical energy density of the simulation box at different fields, obtained by calculating the total energy at different fields and subtracting

off the zero-field total energy. The resulting difference ΔE is negative, indicating a large attraction between the two bounding surfaces. Plotted in Fig. 3 is ΔW , given by ΔE divided by the volume of our simulation sample, as a function of the electric field (red curve). Since the yield stress is directly proportional to ΔW as seen below, all the experimental yield stress vs. electric field data should be able to be scaled onto this relation, if the simulated effect is indeed the GER mechanism.

The electric field at the contact region of two nanoparticles is enhanced by a factor of $\alpha \sim 100\text{-}300$ (compared to the experimentally applied electric field), owing to the large dielectric constant of the nanoparticles and hence the field concentration effect. Thus 0.5 V/nm field in the gap region would correspond roughly to ~ 5000 V/mm (or less) of experimentally applied field. From Fig. 3, we obtain ~ 25 MPa to be the energy density at 0.5 V/nm. This energy density must be scaled by a volume dilution factor β for the energy density of the GER fluid, since the nanoscale gap considered here constitutes the region of closest approach between two nanoparticles. Hence the gap electrical energy should be

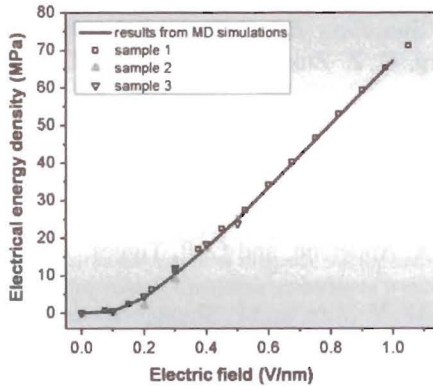


Figure 3. Electrical energy density plotted as a function of applied electric field. Scaled data from three sets of experiments are superposed on the curve. The electric field E is obtained from the measured field E_m by $E = \alpha E_m$, where α is the field enhancement factor (see text for details). The measured yield stress Y is related to the electrical energy density ΔW by $\Delta W = \beta Y / 10$, where β is the volume dilution factor. The values of α and β for samples 1 (Ref.9), 2 (Ref.10) and 3 (Ref.5) are (281.2, 7590), (100, 974), (100, 1010), respectively.

averaged over a volume on the order of d^3 , d being the nanoparticle diameter. For $d \sim 50\text{-}100$ nm and our sample volume of 190 nm^3 , $\beta \sim 1000\text{-}10,000$.

The stress may be expressed as $\tau = (1/\beta)[\partial(\Delta W)/\partial\varepsilon]$, where ε denotes the strain. For a linear stress-strain relation $\tau = a\varepsilon$, it follows that $\Delta W = (\beta/2)a\varepsilon^2$. Here the factor $1/2$ may be replaced by a larger factor if the

stress-strain relation deviates from linearity at large strain values, but such deviations can be absorbed into the β factor. Since yield stress $Y = \tau_y = \alpha \epsilon_o$, we have $Y = \tau_y = 2\Delta W / \beta \epsilon_o$, where $\epsilon_o = 0.2$ (radian) is the strain at the yield point [13]. By suitably scaling the experimental data by α and β values as indicated in the caption to Fig. 3, it is seen that all three data sets fall on the curve obtained from the MD simulations. As the values of α and β fall within the physically reasonable range, our simulation results thus offer a microscopic account of the GER effect.

Acknowledgments

This work is supported by HK Research Grants No. RGC602207 and No. RGC621006. Authors are grateful to the Max Planck Institute for Polymer Research where part of the work was performed.

References

1. R. Tao and J. M. Sun, *Phys. Rev. Lett.* **67**, 398 (1991).
2. D. J. Klingenberg, C. Z. Zukoski, and J. C. Hill, *J. Appl. Phys.* **73**, 4644 (1993).
3. H. Conrad and A. F. Sprecher, *J. Statist. Phys.* **64**, 1073 (1994).
4. H. J. H. Clercx and G. Bossis, *Phys. Rev. E* **52**, 2727 (1995).
5. H. R. Ma, W. Wen, W. Y. Tam, and P. Sheng, *Phys. Rev. Lett.* **77**, 2499 (1996).
6. J. E. Martin, R. A. Anderson, and C. P. Tigges, *J. Chem. Phys.* **110**, 4854 (1999).
7. H. Ma, W. Wen, W. Y. Tam, and P. Sheng, *Adv. in Phys.* **52**, 343 (2003).
8. P. Sheng and W. Wen, *Sol. State Comm.* **150**, 1023 (2010).
9. W. Wen, X. Huang, S. Yang, K. Lu, and P. Sheng, *Nature Materials* **2**, 727 (2003).
10. W. Wen, X. Huang, and P. Sheng, *Appl. Phys. Lett.* **85**, 299 (2004).
11. C. Shen, W. Wen, S. Yang, and P. Sheng, *J. Appl. Phys.* **99**, 106104 (2006).
12. X. Gong et al., *Nanotechnology* **19**, 165602 (2008).
13. X. Huang, W. Wen, S. Yang, and P. Sheng, *Solid State Commun.* **139**, 581 (2006).
14. S. Chen, X. Huang, Nico F. A. van der Vegt, W. Wen and P. Sheng, *Phys. Rev. Lett.* **105**, 046001 (2010).